

Published in final edited form as:

*Mol Cancer Ther.* 2013 July ; 12(7): . doi:10.1158/1535-7163.MCT-12-1185.

## Potential Role of mTORC2 as a Therapeutic Target in Clear Cell Carcinoma of the Ovary

Takeshi Hisamatsu<sup>1,6</sup>, Seiji Mabuchi<sup>1,6,\*</sup>, Yuri Matsumoto<sup>1</sup>, Mahiru Kawano<sup>1</sup>, Tomoyuki Sasano<sup>1</sup>, Ryoko Takahashi<sup>1</sup>, Kenjiro Sawada<sup>1</sup>, Kimihiko Ito<sup>2</sup>, Hirohisa Kurachi<sup>3</sup>, Russell J. Schilder<sup>4</sup>, Joseph R. Testa<sup>5</sup>, and Tadashi Kimura<sup>1</sup>

<sup>1</sup>Department of Obstetrics and Gynecology, Osaka University Graduate School of Medicine. 2-2 Yamadaoka, Suita, Osaka, 565-0871 Japan

<sup>2</sup>Department of Obstetrics and Gynecology, Kansai Rosai Hospital. 3-1-69 Inabaso, Amagasaki, Hyogo, 660-8511 Japan

<sup>3</sup>Department of Obstetrics and Gynecology, Yamagata University Graduate School of Medicine. 2-2-2 Iidanishi, Yamagata, Yamagata 990-9585 Japan

<sup>4</sup>Department of Medical Oncology, Thomas Jefferson University, Philadelphia, PA 19107 USA

<sup>5</sup>Cancer Biology Program, Fox Chase Cancer Center, Philadelphia, PA 19111 USA

### Abstract

The goal of this study was to examine the role of mTORC2 as a therapeutic target in ovarian clear cell carcinoma (CCC), which is regarded as an aggressive, chemoresistant histological subtype.

Using tissue microarrays of 98 primary ovarian cancers (52 CCCs and 46 serous adenocarcinomas (SACs)), activation of mTORC2 was assessed by immunohistochemistry. Then, the growth-inhibitory effect of mTORC2-targeting therapy, as well as the role of mTORC2 signaling as a mechanism for acquired resistance to the mTORC1 inhibitor RAD001 in ovarian CCC, were examined using two pairs of RAD001-sensitive parental (RMG2 and HAC2) and RAD001-resistant CCC cell lines (RMG2-RR and HAC2-RR). mTORC2 was more frequently activated in CCCs than in SACs (71.2% vs. 45.7%). Simultaneous inhibition of mTORC1 and mTORC2 by AZD8055 markedly inhibited the proliferation of both RAD001-sensitive and RAD001-resistant cells *in vitro*. Treatment with RAD001 induced mTORC2-mediated AKT activation in RAD001-sensitive CCC cells. Moreover, increased activation of mTORC2-AKT signaling was observed in RAD001-resistant CCC cells compared to the respective parental cells. Inhibition of mTORC2 during RAD001 treatment enhanced the anti-tumor effect of RAD001 and prevented CCC cells from acquiring resistance to RAD001.

In conclusion, mTORC2 is frequently activated, and can be a promising therapeutic target, in ovarian CCCs. Moreover, mTORC2-targeted therapy may be efficacious in a front-line setting as well as for second-line treatment of recurrent disease developing after RAD001-treatment.

### Keywords

mTORC1; mTORC2; AKT; resistance; ovarian clear cell carcinoma

\*Correspondence to: Seiji Mabuchi, M.D., Ph.D. Department of Obstetrics and Gynecology, Osaka University Graduate School of Medicine, 2-2 Yamadaoka, Suita, Osaka 565-0871, Japan. Telephone: +81-6-6879-3354, FAX: +81-6-6879-3359, smabuchi@gyne.med.osaka-u.ac.jp.

<sup>6</sup>These authors contributed equally to this work.

**Conflicts of interest statement:** The authors declare that they have no conflicts of interest.

## Introduction

The mammalian target of rapamycin (mTOR) is a serine/threonine kinase that plays a key role in cell growth and proliferation (1). In cells, mTOR resides in at least two functionally distinct complexes, mTOR Complex 1 (mTORC1) and mTOR Complex 2 (mTORC2). mTORC1 phosphorylates the translation-regulating factors S6K-1 (ribosomal S6 kinase-1) and 4EBP-1 (eukaryote translation initiation factor 4E binding protein-1), and regulate a variety of processes including proliferation, motility, differentiation, survival, autophagy, angiogenesis, and metabolism in response to nutrients or growth factor signals (1). The more recently identified mTORC2 phosphorylates the survival kinase AKT, protein kinase C alpha and SGK1, leading to regulation of the actin cytoskeleton network (2).

Frequent mTOR activation in human epithelial ovarian cancer was first described in a 2004 report, in which AKT-mTORC1 signaling was shown to be activated in 55% of epithelial ovarian cancers (3). A subsequent preclinical study specifically targeting ovarian clear cell carcinoma (CCC), a chemoresistant histological subtype of epithelial ovarian cancer, revealed that mTORC1 is more frequently activated in CCC than in the more common subtype, serous adenocarcinoma (SAC): 86.6% vs. 50%, respectively (4). This finding may be explained by the recent finding that activating mutations of *PIK3CA* occur more frequently in CCC than in any other histological subtypes of epithelial ovarian cancer (5), suggesting that patients with CCC may be more responsive to mTORC1-targeted therapy (6,7). Given that patients with CCC have poor prognosis due mainly to the lack of effective chemotherapy (8,9), hopes are high for the development of mTOR-targeting therapy in this patient population (10).

Rapamycin and its analogs (rapalogs) are all highly specific inhibitors of mTORC1. The rapalogs inhibit mTORC1 by first binding to the intracellular protein FK506 binding protein 12 (FKBP12). The resulting mTOR inhibitor-FKBP12 complex then binds to mTOR at the FKBP12-rapamycin-binding domain (FRB), thereby inhibiting the serine/threonine kinase activity of mTORC1 by an allosteric mechanism (11). Although rapalogs have demonstrated significant growth-inhibitory effects on a variety of human malignancies, it is increasingly recognized that the mechanism of action of rapalogs may not be sufficient for achieving a broad and robust anticancer effect due to their inability to inhibit mTORC2 activity (12). In fact, in a phase III clinical study, renal cell carcinoma patients treated with everolimus experienced disease progression with a median progression free interval of only 4 months (13).

In ovarian cancer, although the role of mTORC1 as a therapeutic target has been intensively investigated preclinically (4, 14–17), the mechanism responsible for resistance to mTORC1 inhibitors has not been reported previously. Moreover, with regard to mTORC2, only limited *in vitro* information is available (18).

In this report, we examine the involvement of mTORC2 activation in both early stage and advanced stage ovarian CCC and its possible role as a therapeutic target. We also evaluate the role of mTORC2 as a mechanism for acquired resistance to the mTORC1 inhibitor RAD001 in CCC cells. Finally, we investigate whether inhibition of mTORC2 activity can prevent CCC cells from acquiring resistance to RAD001.

## Materials and Methods

### Reagents/antibodies

RAD001 was obtained from Novartis Pharma AG (Basel, Switzerland). AZD8055 was purchased from Selleck Chemicals (Houston, TX). Enhanced chemiluminescence Western blotting detection reagents were from Perkin Elmer (Waltham, MA). Antibodies recognizing Rictor, phospho-Rictor (Thr1135), S6K1, phospho-S6K1 (Thr389), AKT, phospho-AKT (Ser473), PRAS40, phospho-PRAS40 (Thr246), 4EBP1, phospho-4EBP1 (Thr37/46), and  $\beta$ -actin were obtained from Cell Signaling Technology (Beverly, MA). Anti-rabbit secondary antibodies were purchased from Santa Cruz Biotechnology (Santa Cruz, CA). The Cell Titer 96-well proliferation assay kit was obtained from Promega (Madison, WI).

### Cell lines and culture

Human ovarian CCC cell lines RMG1, RMG2, KOC7C, and HAC2 were kindly provided by Dr. H. Itamochi (Tottori University, Tottori, Japan). These cell lines were extensively characterized previously (19–24). We tested these cell lines in our laboratory for its authentication by morphologic observation. No further cell line authentication was conducted by the authors. Each cell line was never continuously passaged in culture for more than 3 months, and after that, a new vial of frozen cells was thawed. These cells were cultured in DMEM/Ham's F-12, (Gibco, Carlsbad, CA) with 10% fetal bovine serum, as reported previously (4,14,24).

### Determination of cell number

CCC cells were seeded into 96-well plates at a density of  $3 \times 10^3$ /well. The monolayers were washed once with PBS, the cells were detached with trypsin, and viable cells were counted by trypan blue dye exclusion.

### Establishment of RAD001-resistant cell lines

RAD001-resistant sublines from RMG2 and HAC2 were developed by continuous exposure to RAD001 (Supplemental Fig. 1). Briefly, cells of both lines were exposed to stepwise increases in RAD001 concentration. Initial RAD001 exposure was at a concentration of 1 nM. After the cells had regained their exponential growth rate, the RAD001 concentration was doubled and then the procedure was repeated until selection at 1  $\mu$ M was attained. The resulting RAD001-resistant sublines, designated as RMG2-RR and HAC2-RR, were cultured in DMEM containing 1  $\mu$ M RAD001 to maintain a high level of RAD001-resistance.

### Cell proliferation assay

A MTS assay was used to analyze the effect of RAD001 or AZD8055 on cell viability as described (25). Cells were cultured overnight in 96-well plates ( $1 \times 10^4$  cells/well). Cell viability was assessed after addition of RAD001 or AZD8055. The number of surviving cells was assessed by determination of the  $A_{490\text{ nm}}$  of the dissolved formazan product after addition of MTS.

### Cell cycle analysis

Cells were incubated with 10 nM RAD001 or 10 nM AZD8055 for 48 h. Cells were then fixed with 75% ethanol, and stained with propidium iodide (50  $\mu$ g/ml) in the presence of RNase A (100  $\mu$ g/ml; Roth, Karlsruhe, Germany) for 20 min at 4°C. Cell cycle distribution was determined by analyzing 10,000 cells using a FACScan flow cytometer and Cell Quest software (Becton Dickinson, San Jose, CA) as reported elsewhere (15).

### ***In vitro* detection of apoptosis**

Cells were treated with 10 nM RAD001 or 10 nM AZD8055 for 24 h in the presence of 5% FBS. In brief, cells were lysed and DNA fragmentation was detected using a Cell Death Detection ELISA Kit (Roche, Penzberg, Germany) per the manufacturer's instructions.

### **Western blot analysis**

Cells treated as indicated were lysed for 10 min at 4°C. Equal amounts of proteins were separated by SDS-PAGE and transferred to nitrocellulose membranes. Western blot analyses were performed using various specific primary antibodies. Immunoblots were visualized with horseradish peroxidase-coupled immunoglobulin by using an enhanced chemiluminescence Western blotting system (Perkin Elmer, Boston, MA).

### **mTORC2 kinase assays**

Kinase assays of endogenous mTORC2 were performed as described previously (26). The cells were lysed on ice for 10 min in 1 ml lysis buffer. After centrifugation, the supernatant was incubated with anti-Rictor antibody at 4 °C for 12 h, followed by incubation with protein A-agarose for another 2 h. Immunocomplexes were incubated in kinase reaction buffer containing 50 ng of inactive AKT and 50 μM ATP for 30 min at 37 °C. The reaction was terminated by adding 6×SDS sample buffer, and AKT phosphorylation was detected by Western blotting.

### **RNA interference**

The siRNA specifically targeting S6K1 (catalog #sc-36165) and a nontargeting control siRNA (catalog #sc-37007) were purchased from Santa Cruz Biotechnology (Santa Cruz, CA). The shRNA specifically targeting Rictor (catalog #TG307650) and a nontargeting control shRNA (catalog #TR30013) were purchased from Origene (Rockville, MD). RMG2 and HAC2 cells incubated in 6-well plates were transfected with siRNA or shRNA using Lipofectamine 2000 (Invitrogen, Carlsbad, CA). Transiently-transfected cells were assayed 48 h post transfection. The shRNA plasmids carried a kanamycin resistance gene that permits the selection of stable transfectants. Clonal selection was performed by adding kanamycin (Sigma, St. Louis, MO) into the medium ~24 h after transfection. The resulting stable transfectants expressing control shRNA or Rictor shRNA were designated as cell lines RMG2-control, RMG2-RictorKD, HAC2-control, and HAC2-RictorKD.

### **Clinical samples**

All surgical specimens including ovarian cancers and normal ovaries were collected and archived according to protocols approved by the institutional review boards of the parent institutions. Appropriate informed consent was obtained from each patient. The tumors included 46 SACs and 52 CCCs. Based on criteria of the International Federation of Gynecology and Obstetrics (FIGO), 22 SACs were stage I–II tumors and 24 were stage III–IV tumors. Among CCCs, 27 were stage I–II and 25 were stage III–IV.

### **Immunohistochemistry**

Tumor samples were fixed in 10% neutral buffered formalin overnight and then embedded in paraffin. Ovarian cancer tissue microarrays consisting of two cores from each tumor sample were prepared by the Tumor Bank Facility at Fox Chase Cancer Center, as described previously (4,24). Tissue sections were cut at 4 μm, mounted on slides, and processed for immunohistochemical staining. Sections were incubated with the primary antibody, followed by the appropriate peroxidase-conjugated secondary antibody.

The slides were scored semiquantitatively by two pathologists who were blinded to the clinical outcome. Surrounding non-neoplastic stroma served as an internal negative control for each slide. A score of 0 indicated no staining, +0.5 was weak focal staining (<10% of the cells stained), +1 was indicative of focal staining (10–50% of the cells stained), +2 indicated clearly positive staining (>50% of the cells stained), and a score of +3 was intensely positive. Tumors with +0.5 or +1 were combined and designated as the weak-staining group. Tumors with staining of +2 or +3 comprised the medium-staining and strong-staining groups, respectively. When the two cores from the same tumor sample showed different positivity results, the lower score was considered valid.

### ***In vivo* tumor studies**

All procedures involving animals and their care were approved by the Institutional Animal Care and Usage Committee of Osaka University, in accordance with institutional and NIH guidelines. Five to seven-week-old nude mice (n = 40) were inoculated s.c. into the right flank either with  $5 \times 10^6$  RMG2-control, RMG2-RictorKD, HAC2-control, or HAC2-RictorKD cells in 200  $\mu$ l of PBS, with 10 mice in each group. When tumors reached about 50 mm<sup>3</sup>, the mice were assigned into two treatment groups: placebo (n=5) or 2.5 mg/kg RAD001 (n=5), with treatment given every 2 days. RAD001 was administered intragastrically using an animal-feeding needle. Caliper measurements of the longest perpendicular tumor diameters were done every week to estimate tumor volume using the following formula:  $V = L \times W \times D \times \pi/6$ , where V is the volume, L is the length, W is the width, and D is the depth.

### **Statistical analysis**

The effect of mTOR inhibition on cell proliferation and apoptosis was analyzed by Student's T test. Tumor volume was analyzed by Wilcoxon exact test. Immunoreactivity was analyzed using Fisher's exact test. Spearman's correlation coefficient with confidence interval (CI) was calculated to assess the relationship between phospho-mTOR (Ser2481) immunoreactivity and phospho-AKT immunoreactivity.

## **Results**

### **mTORC2 is expressed and more frequently activated in CCCs than in SACs**

Phosphorylation of mTOR at Ser2481 has been reported to be a marker for mTORC2 activation (27, 28). To determine the expression and activation of mTORC2, tissue microarrays and normal ovarian tissues were examined immunohistochemically for phospho-mTOR (Ser2481) and Rictor, an essential component of mTORC2. As shown in Figure 1A, B and Supplemental Table 1, significantly stronger immunoreactivity for phospho-mTOR (Ser2481) was observed in CCCs and SACs than in ovarian surface epithelial cells. Rictor expression was observed in both ovarian cancers and normal ovarian tissues. Although CCCs with SACs exhibited no differences in immunoreactivity for Rictor, significantly stronger immunoreactivity for phospho-mTOR (Ser2481) was observed in CCCs than in SACs. Among the 46 SACs, 25 (54.3%) showed negative/weak staining and 21 (45.7%) showed medium staining. No SAC had strong expression of phospho-mTOR (Ser2481). In contrast, among the 52 CCCs, 15 tumors (28.8%) had negative/weak staining, 25 (48.1%) showed medium staining, and 12 (23.1%) stained strongly. The frequency of medium/strong phospho-mTOR immunoreactivity was significantly higher in CCCs than in SACs (71.2% and 45.7%, respectively). When analyzed by clinical stage, as shown in Fig. 1C, medium/strong phospho-mTOR (Ser2481) expression was observed in 76% of advanced stage CCCs and in 66.7% of early stage CCCs, compared to 40.9% and 50.0% in advanced stage and early stage SACs, respectively. Collectively, these results indicate that mTORC2

is frequently expressed and activated in CCCs than in SACs, especially those in advanced stage disease.

mTORC2 is known to phosphorylate AKT at Ser 473, and thus, AKT phosphorylation has also been used as a marker for mTORC2 activation (12). To determine if mTOR phosphorylation at Ser2481 in our CCCs paralleled AKT phosphorylation (Ser473), immunohistochemical analysis was performed, and the immunoreactivity was scored semiquantitatively. In total, 28 of 52 (53.8%) CCCs showed significant expression of both phospho-AKT (Ser473) and phospho-mTOR (Ser2481) and 10 of 52 (19.2%) tumors showed phosphorylation of neither AKT nor mTOR (Table 1). Altogether, an association between phospho-AKT (Ser473) staining and phospho-mTOR (Ser2481) staining was observed in 38 of 52 ovarian tumors (73.1%). Statistical assessment revealed that the phospho-mTOR (Ser2481) immunoreactivity correlated positively with phospho-AKT immunoreactivity (Spearman's correlation coefficient,  $r = 0.604$ ,  $p < 0.0001$ ).

### ***In vitro* growth-inhibitory effect of AZD8055 on CCC cell lines**

Given the frequent mTORC2 activation found in human CCC tumor specimens (Fig. 1A–C), we evaluated the activation of mTORC2 in four human CCC cell lines by *in vitro* kinase assay. As shown in Fig. 1D, under serum-starvation conditions, Rictor expression and mTORC2 activation are observed in all CCC cell lines tested, which is consistent with immunohistochemical results observed with tumor samples.

Using these cell lines, we examined the anti-tumor effect of mTORC2-targeting therapy *in vitro*. For this purpose, we employed the mTOR kinase inhibitor AZD8055, which has been shown to inhibit both mTORC1 and mTORC2, and compared its efficacy with that of the mTORC1 inhibitor RAD001, which is used clinically as everolimus (Fig. 2A). As shown in Fig. 2B, AZD8055 exhibited more robust antiproliferative activity than RAD001, with ~80% inhibition at the highest drug concentration tested, which was significantly greater than ~40% of growth inhibition observed in cells treated with RAD001.

We next examined the effect of AZD8055 on cell cycle progression by flow cytometry. As shown in Supplemental Table 2, treatment of both RMG2 and HAC2 cells with 10 nM AZD8055 resulted in a slight increase in the percentage of cells in G1 phase compared to that seen with RAD001. Moreover, as shown, with both cell lines the percentage of apoptotic cells in sub-G1 was also significantly increased after treatment with AZD8055 (Supplemental Table 2), which is consistent with the result of an ELISA assay showing apoptosis being observed in AZD8055-treated cells (Fig. 2C). Treatment with RAD001 did not induce apoptosis in either cell line (Supplemental Table 2, Fig. 2C). Collectively, these results suggest that AZD8055 inhibits proliferation of CCC cells by inducing both cell cycle arrest and apoptosis.

We further examined the effect of AZD8055 and RAD001 on the phosphorylation of S6K1 (Thr389), 4EBP1 (Thr37/46), and AKT (Ser473) in RMG2 and HAC2 cells. As shown in Fig. 2D, treatment with AZD8055 greatly inhibited the phosphorylation of these molecules. In contrast, although treatment with RAD001 potently inhibited S6K1, it could not inhibit the phosphorylation of 4EBP1 (Thr37/46) and AKT (Ser473). In fact, RAD001 was found to induce phosphorylation of AKT. It has been reported that the greater inhibition of 4EBP1 at T37/46 is associated with a greater inhibition of cap-dependent translation and cellular proliferation (29). Thus, the greater anti-tumor effect of AZD8055 than RAD001 observed in CCC cells may be explained, at least in part, by the effect of AZD8055 on AKT and 4EBP1. Altogether, these results strongly suggest that mTORC2 is a promising therapeutic target for the management of CCCs.

### **mTORC1 inhibition by RAD001 induces activation of the AKT signaling pathway**

To further investigate the role of mTORC2 in CCC cells, we next examined whether or not mTORC2 plays a mechanistic role in the resistance to mTORC1 inhibition. For this purpose, we first examined the effect of RAD001 treatment on AKT, a known mTORC2 substrate. As shown in Fig. 3A, treatment with RAD001 induced a modest increase in the phosphorylation of AKT and proline-rich AKT substrate of 40 kDa (PRAS40). In contrast, S6K1 phosphorylation was completely inhibited in both cell lines in response to RAD001 treatment.

PRAS40 is known for its ability to negatively regulate mTORC1 kinase activity (30). Recent investigations suggest that the phosphorylation of PRAS40 by AKT results in the dissociation of PRAS40 from mTORC1 and may relieve an inhibitory constraint on mTORC1 activity (30). Thus, our *in vitro* data suggests that mTORC1 inhibition by RAD001 triggers a negative feedback mechanism resulting in activation of AKT-PRAS40 signaling, which may attenuate the anti-tumor effect of RAD001 in CCC cells.

### **Induction of AKT-PRAS40 phosphorylation after mTORC1 inhibition requires mTORC2**

It has been previously reported that mTORC2-mediated activation of AKT is involved in the mechanism responsible for resistance to rapamycin in diffuse large B-cell lymphoma (31). However, whether this mechanism is cell type specific or whether these preclinical findings are of clinical relevance is unknown.

To determine the mechanism by which RAD001 induces AKT phosphorylation in CCC cells, we used both a mTOR kinase inhibitor (AZD8055) and shRNA against the mTORC2 component Rictor. As shown in Fig. 2D, treatment with RAD001 for 3 h induced phosphorylation of AKT. However, such AKT phosphorylation was not observed in response to simultaneous inhibition of mTORC1 and mTORC2 by AZD8055, indicative of the involvement of mTORC2 in mTORC1 inhibition-mediated activation of AKT in CCC cells.

To further examine the role of mTORC2 in RAD001-induced AKT S473 phosphorylation, cells were transiently transfected with shRNA against Rictor before treating with RAD001. As shown in Fig. 3B, specific knockdown of Rictor caused a reduction in the basal level of Rictor and in the phosphorylation of AKT and PRAS40. Collectively, these data indicate that AKT phosphorylation following mTORC1 inhibition in CCC cells is mediated in a mTORC2-dependent manner and can be blocked by mTORC2 inhibition.

We further investigated the mechanism by which mTORC2 is activated in response to RAD001 treatment. A recent report demonstrated that S6K1 directly phosphorylates Rictor on Thr1135, negatively regulating the ability of mTORC2 to phosphorylate AKT (32). As shown in Fig. 3A, treatment of CCC cells with RAD001 attenuated the phosphorylation of S6K1 and Rictor (Thr1135) in a time dependent manner, which sharply contrasts with the increased phosphorylation of AKT seen following RAD001 treatment. Moreover, specific knockdown of S6K1 by siRNA attenuated the phosphorylation of Rictor (Thr1135), which resulted in increased activation of mTORC2 (Figure 3C). These results imply that RAD001-induced mTORC2 activation occurs by attenuating S6K1-mediated Rictor phosphorylation (Fig. 3D).

### **mTORC2-AKT activation is responsible for resistance to RAD001**

To investigate whether mTORC1 inhibition-mediated mTORC2 activation is linked mechanistically to RAD001 resistance, we established RAD001-resistant cell lines from RMG2 and HAC2 cells (Supplemental Fig. 1). We next examined the activity of mTORC2

in both RAD001-resistant sublines and parental RAD001-sensitive cells by *in vitro* kinase assay. As shown in Fig. 4A, greater activation of mTORC2 was observed in the RAD001-resistant sublines compared to the respective parental cell lines. We also investigated AKT-PRAS40 signaling in both RAD001-resistant sublines and parental cells by Western blotting. As shown in Fig. 4B, significantly higher phospho-AKT and phospho-PRAS40 expression levels were observed in both RAD001-resistant sublines relative to the respective parental cell lines.

We next investigated whether the hyperphosphorylation of AKT-PRAS40 signaling observed in RAD001-resistant CCC cells is mediated by mTORC2. As shown in Fig. 4C, knockdown of Rictor resulted in attenuated phosphorylation of AKT and PRAS40 in RAD001-resistant CCC cells. Similarly, treatment with AZD8055 inhibited the phosphorylation of both AKT and PRAS40 in RAD001-resistant CCC cells (Fig. 4D). Collectively, our results indicate that the hyperphosphorylation of AKT observed in RAD001-resistant CCC cells is mediated by mTORC2 and that RAD001 resistance is mediated, at least in part, by activation of mTORC2-AKT signaling in CCC cells.

### **Inhibition of mTORC2 prevents CCC cells from acquiring resistance to RAD001**

We next examined whether continuous inhibition of mTORC2 during the course of RAD001 treatment *in vivo* can prevent CCC cells from acquiring resistance to RAD001. For this purpose, we established cell lines stably expressing Rictor shRNA. As shown in Fig. 5A, CCC cells expressing Rictor shRNA (RMG2-RictorKD cells and HAC2-RictorKD cells) had significantly reduced levels of Rictor compared with control cells. Using these cell lines, we first examined the *in vitro* growth-inhibitory effect of RAD001. As shown in Figure 5B, although both RMG2-control cells and HAC2-control cells showed sensitivity to RAD001 treatment at day 3, the cells started to proliferate again thereafter, resulting in an increased number of cells at day 7. In contrast, in RMG2-RictorKD cells and HAC2-RictorKD cells, RAD001 treatment decreased the number of viable CCC cells in a time dependent manner, resulting in almost 90% disappearance of CCC cells at day 7. We then determined the effect of RAD001 on the *in vivo* growth of RMG2-RictorKD- and HAC2-RictorKD-derived tumors. As shown in Fig. 5C, in mice treated with placebo, the RMG2-RictorKD-derived tumor was significantly smaller than that of RMG2-control derived tumor, indicating that knockdown of Rictor inhibits the *in vivo* growth of CCC cells. When the mice were treated with RAD001, clear differential sensitivity to RAD001 was observed between RMG2-RictorKD-derived tumors and control RMG2-control derived tumors. Moreover, RAD001 treatment showed long-lasting anti-tumor effects on tumors derived from RMG2-RictorKD cells. Similar results were observed in mice inoculated with HAC2-RictorKD or HAC2-control cells. Together, these results indicate that inhibition of mTORC2 activity during RAD001 treatment enhances the therapeutic efficacy of RAD001 and prevented CCC cells from acquiring resistance to RAD001.

We finally determined the growth-inhibitory effect of AZD8055 in RAD001-resistant CCC cells. As shown in Figure 5D, in contrast to the effect of the mTORC1 inhibitor RAD001, simultaneous inhibition of mTORC1 and mTORC2 by treatment with AZD8055 inhibited the proliferation of RAD001-resistant CCC cells in a dose-dependent manner. This finding indicates that simultaneous inhibition of mTORC1 and mTORC2 might be efficacious in CCC patients who become resistant to RAD001 therapy.

## **Discussion**

Clear cell carcinoma (CCC) of the ovary is a distinctive subtype of epithelial ovarian cancer associated with a poorer sensitivity to platinum-based chemotherapy and a worse prognosis than more common serous adenocarcinomas both in front-line and recurrent settings



(8,9,33). Therefore, to improve survival of CCC patients, novel treatment strategies need to be developed.

Previous investigations indicated that mTORC1 is frequently activated in CCC of the ovary and *in vitro* studies suggested that mTORC1 can be targeted therapeutically (4,17). On the basis of promising results from preclinical and clinical investigations (4,17,34), the Gynecologic Oncology Group (GOG) is currently conducting a phase II trial (protocol GOG0268) designed to evaluate the efficacy of temsirolimus in combination with carboplatin+paclitaxel as a first-line chemotherapy in patients with stage III–IV CCC of the ovary (7). In addition, for patients with recurrent CCC of the ovary, the Japanese Gynecologic Oncology Group (JGOG) will soon initiate a phase II trial of everolimus monotherapy in their protocol JGOG3012.

Compared to mTORC1, the role of mTORC2 as a therapeutic target in CCC of the ovary has not been previously documented. However, there is emerging evidence for a role for mTORC2 as an important driver for tumorigenesis. It has been reported that exogenous overexpression of Rictor promotes mTORC2 activity, increases proliferative and invasive potential of cancer cells (35), and induces malignant tumors in mice (36). In this investigation, we found that Rictor, an essential component of the mTORC2 complex, is frequently expressed in CCC of the ovary. Expression of phospho-mTOR (Ser 2481), a reported marker of mTORC2 activation, is more frequently expressed in CCCs than in SACs (71.2% versus 45.7%, respectively). While the mechanism by which mTORC2 is activated in CCC is unknown, our results suggest that mTORC2 plays an important role in the development of CCC and represents a viable therapeutic target in this disease.

AZD8055 is an orally bioavailable mTOR kinase inhibitor that is currently being evaluated in phase I/II clinical studies in a variety of solid tumors. AZD8055 binds to the mTOR kinase domain and directly affects both mTORC1 and mTORC2 kinase activity. Thus, AZD8055 theoretically would be expected to have a more profound effect on mTOR signaling than rapalogs that target only mTORC1 (37). As shown in Fig. 2B and C, treatment with AZD8055 had more robust anti-tumor activity than RAD001 in RAD001-sensitive CCC cells, with  $IC_{50}$  values in a low nanomolar range. This finding may be explained, at least in part, by AZD8055's ability to inhibit phosphorylation of 4EBP1 at Thr37/46 (Fig. 2D), which has been reported to be associated with a greater inhibition of cap-dependent translation and cellular proliferation (29). Taken together, these results indicate that not only mTORC1, but also mTORC2, are rational targets for the treatment of CCC of the ovary.

The precise mechanism responsible for acquired resistance to mTORC1 inhibitors remains unknown. Both mTORC2-mediated AKT activation and mTORC2-independent, IRS1-dependent AKT activation in response to mTORC1 inhibition has been proposed as possible mechanisms (38, 39). However, whether these mechanisms are cell type specific or whether these preclinical findings are of clinical relevance in ovarian CCC, have not been previously addressed. In this study, we have demonstrated that RAD001-resistant CCC sublines exhibit enhanced AKT and PRAS40 phosphorylation compared to parental RAD001-sensitive cell lines (Fig. 4B). Moreover, treatment with RAD001 induced phosphorylation of both AKT and PRAS40 in RAD001-sensitive CCC cells (Fig. 2D and 3A). These findings are consistent with previous work showing that rapamycin treatment induces an increase in AKT and PRAS40 phosphorylation in a subset of patients with PTEN-deficient glioblastoma and that this increased PRAS40 phosphorylation was associated with shorter survival (40). As shown in Fig. 3, the increased phosphorylation of AKT-PRAS40 was associated with activation of mTORC2, which was induced by decreased phosphorylation of Rictor in response to RAD001 treatment. Moreover, inhibition of mTORC2 activity by knockdown of

Rictor during RAD001 treatment prevented RMG1 cells from acquiring resistance to RAD001 (Fig. 5B). Collectively, these results indicate that the Rictor-mTORC2-AKT-PRAS40 feedback loop induced by RAD001 treatment is, at least in part, responsible for acquired resistance to RAD001 (Fig. 3D).

An additional important finding in our study is the potent anti-tumor activity of AZD8055 in RAD001-resistant CCC (Fig. 5D). Given that renal cell carcinoma patients treated with everolimus experienced disease progression with a median progression free interval of 4 months in a phase III study (13), it is of great importance to explore the salvage treatment for recurrent tumors developed after everolimus treatment. Our results suggest that mTOR inhibitors that inhibit both mTORC1 and mTORC2 might be efficacious for the clinical management of recurrent CCCs developed after the treatment with a mTORC1 inhibitor such as RAD001.

In summary, our results indicate that mTORC2 is frequently activated in ovarian CCC and is a promising therapeutic target for this disease both as a front-line treatment and as a salvage treatment for recurrence after everolimus treatment. This work provides scientific rationale for future clinical trials of mTORC2-targeting therapies in patients with ovarian CCC, a chemoresistant histological subtype characterized by frequent hyperactivation of the mTOR complexes.

## Supplementary Material

Refer to Web version on PubMed Central for supplementary material.

## Acknowledgments

Grant support: S. Mabuchi is supported in part by grant-in-aid for General Scientific Research, no. 23592446, from the Ministry of Education, Culture, Sports, Science and Technology of Japan. H. Kurachi is supported in part by grant-in-aid for General Scientific Research, no. 22390308, from the Ministry of Education, Culture, Sports, Science and Technology of Japan. J.R. Testa received support from NCI grant CA77429.

We thank Drs. Y. Nishio, M. Tsujimoto, M. Ohmichi, Y. Terai, M. Yamoto and Y. Tsubota for providing tumor specimens and clinical information.

## Abbreviations

<b>CCC</b>	clear cell carcinoma
<b>SAC</b>	serous adenocarcinoma
<b>mTOR</b>	mammalian target of rapamycin
<b>S6K1</b>	S6 kinase 1
<b>4EBP1</b>	eIF4E binding protein 1
<b>PRAS40</b>	proline-rich AKT substrate of 40 kDa
<b>IHC</b>	immunohistochemistry
<b>shRNA</b>	small hairpin RNA
<b>IGF</b>	insulin-like growth factor
<b>IRS</b>	insulin receptor substrate
<b>ELISA</b>	Enzyme-Linked ImmunoSorbent Assay

## References

1. Laplante M, Sabatini DM. mTOR signaling in growth control and disease. *Cell*. 2012; 149:274–93. [PubMed: 22500797]
2. Wander SA, Hennessy BT, Slingerland JM. Next-generation mTOR inhibitors in clinical oncology: how pathway complexity informs therapeutic strategy. *J Clin Invest*. 2011; 121:1231–41. [PubMed: 21490404]
3. Altomare DA, Wang HQ, Skele KL, De Rienzo A, Klein-Szanto AJ, Godwin AK, et al. AKT and mTOR phosphorylation is frequently detected in ovarian cancer and can be targeted to disrupt ovarian tumor cell growth. *Oncogene*. 2004; 23:5853–7. [PubMed: 15208673]
4. Mabuchi S, Kawase C, Altomare DA, Morishige K, Sawada K, Hayashi M, et al. mTOR is a promising therapeutic target both in cisplatin-sensitive and cisplatin-resistant clear cell carcinoma of the ovary. *Clin Cancer Res*. 2009; 15:5404–13. [PubMed: 19690197]
5. Kuo KT, Mao TL, Jones S, Veras E, Ayhan A, Wang TL, et al. Frequent activating mutations of PIK3CA in ovarian clear cell carcinoma. *Am J Pathol*. 2009; 174:1597–601. [PubMed: 19349352]
6. Mabuchi S, Hisamatsu T, Kimura T. Targeting mTOR signaling pathway in ovarian cancer. *Curr Med Chem*. 2011; 18:2960–8. [PubMed: 21651485]
7. ClinicalTrials.gov. A Service of the U.S. National Institute of Health; NCT 01196429. <http://www.clinicaltrials.gov> [Accessed August 30, 2012]
8. Winter WE 3rd, Maxwell GL, Tian C, Carlson JW, Ozols RF, Rose PG, et al. Prognostic factors for stage III epithelial ovarian cancer: a Gynecologic Oncology Group Study. *J Clin Oncol*. 2007; 25:3621–7. [PubMed: 17704411]
9. Crotzer DR, Sun CC, Coleman RL, Wolf JK, Levenback CF, Gershenson DM. Lack of effective systemic therapy for recurrent clear cell carcinoma of the ovary. *Gynecol Oncol*. 2007; 105:404–8. [PubMed: 17292461]
10. Del Carmen MG, Birrer M, Schorge JO. Clear cell carcinoma of the ovary: A review of the literature. *Gynecol Oncol*. 2012; 126:481–90. [PubMed: 22525820]
11. Sabatini DM. mTOR and cancer: insights into a complex relationship. *Nat Rev Cancer*. 2006; 6:729–34. [PubMed: 16915295]
12. Bhagwat SV, Crew AP. Novel inhibitors of mTORC1 and mTORC2. *Curr Opin Investig Drugs*. 2010; 11:638–45.
13. Motzer RJ, Escudier B, Oudard S, Hutson TE, Porta C, Bracarda S, et al. Efficacy of everolimus in advanced renal cell carcinoma: a double-blind, randomised, placebo-controlled phase III trial. *Lancet*. 2008; 372:449–56. [PubMed: 18653228]
14. Mabuchi S, Hisamatsu T, Kawase C, Hayashi M, Sawada K, Mimura K, et al. The activity of trabectedin as a single agent or in combination with everolimus for clear cell carcinoma of the ovary. *Clin Cancer Res*. 2011; 17:4462–73. [PubMed: 21622721]
15. Mabuchi S, Altomare DA, Cheung M, Zhang L, Poulikakos PI, Hensley HH, et al. RAD001 inhibits human ovarian cancer cell proliferation, enhances cisplatin-induced apoptosis, and prolongs survival in an ovarian cancer model. *Clin Cancer Res*. 2007; 13:4261–70. [PubMed: 17634556]
16. Mabuchi S, Altomare DA, Connolly DC, Klein-Szanto A, Litwin S, Hoelzle MK, et al. RAD001 (Everolimus) delays tumor onset and progression in a transgenic mouse model of ovarian cancer. *Cancer Res*. 2007; 67:2408–13. [PubMed: 17363557]
17. Miyazawa M, Yasuda M, Fujita M, Kajiwara H, Hirabayashi K, Takekoshi S, et al. Therapeutic strategy targeting the mTOR-HIF-1 $\alpha$ -VEGF pathway in ovarian clear cell adenocarcinoma. *Pathol Int*. 2009; 59:19–27. [PubMed: 19121088]
18. Montero JC, Chen X, Ocaña A, Pandiella A. Predominance of mTORC1 over mTORC2 in the regulation of proliferation of ovarian cancer cells: therapeutic implications. *Mol Cancer Ther*. 2012; 11:1342–52. [PubMed: 22496482]
19. Nozawa S, Tsukazaki K, Sakayori M, Jeng CH, Iizuka R. Establishment of a human ovarian clear cell carcinoma cell line (RMG-I) and its single cell cloning--with special reference to the stem cell of the tumor. *Hum Cell*. 1988; 1:426–35. [PubMed: 3154025]

20. Nozawa S, Yajima M, Sasaki H, Tsukazaki K, Aoki D, Sakayori M, et al. A new CA125-like antigen (CA602) recognized by two monoclonal antibodies against a newly established ovarian clear cell carcinoma cell line (RMG-II). *Jpn J Cancer Res.* 1991; 82:854–61. [PubMed: 1715339]
21. Tomioka Y. Establishment and characterization of three human ovarian clear cell carcinoma cell line. *J Kurume Med Assoc.* 1998; 61:323–333.
22. Takemoto Y, Yano H, Momosaki S, Ogasawara S, Nishida N, Kojiro S, et al. Antiproliferative effects of interferon-alphaCon1 on ovarian clear cell adenocarcinoma in vitro and in vivo. *Clin Cancer Res.* 2004; 10:7418–26. [PubMed: 15534119]
23. Niimi S, Nakagawa K, Sugimoto Y, Nishio K, Fujiwara Y, Yokoyama S, et al. Mechanism of cross-resistance to a camptothecin analogue (CPT-11) in a human ovarian cancer cell line selected by cisplatin. *Cancer Res.* 1992; 52:328–33. [PubMed: 1345810]
24. Mabuchi S, Kawase C, Altomare DA, Morishige K, Hayashi M, Sawada K, et al. Vascular endothelial growth factor is a promising therapeutic target for the treatment of clear cell carcinoma of the ovary. *Mol Cancer Ther.* 2010; 9:2411–22. [PubMed: 20663925]
25. Mabuchi S, Ohmichi M, Nishio Y, Hayasaka T, Kimura A, Ohta T, et al. Inhibition of NFkappaB increases the efficacy of cisplatin in vitro and in vivo ovarian cancer models. *J Biol Chem.* 2004; 279:23477–85. [PubMed: 15026414]
26. Huang J. An in vitro assay for the kinase activity of mTOR complex 2. *Methods Mol Biol.* 2012; 821:75–86. [PubMed: 22125061]
27. Copp J, Manning G, Hunter T. TORC-specific phosphorylation of mammalian target of rapamycin (mTOR): phospho-Ser2481 is a marker for intact mTOR signaling complex 2. *Cancer Res.* 2009; 69:1821–7. [PubMed: 19244117]
28. Carayol N, Vakana E, Sassano A, Kaur S, Goussetis DJ, Glaser H, et al. Critical roles for mTORC2- and rapamycin-insensitive mTORC1-complexes in growth and survival of BCR-ABL-expressing leukemic cells. *Proc Natl Acad Sci U S A.* 2010; 107:12469–74. [PubMed: 20616057]
29. Proud CG. mTORC1 signalling and mRNA translation. *Biochem Soc Trans.* 2009; 37:227–31. [PubMed: 19143637]
30. Wang H, Zhang Q, Wen Q, Zheng Y, Philip L, Jiang H, et al. Proline-rich Akt substrate of 40kDa (PRAS40): a novel downstream target of PI3k/Akt signaling pathway. *Cell Signal.* 2012; 24:17–24. [PubMed: 21906675]
31. Gupta M, Ansell SM, Novak AJ, Kumar S, Kaufmann SH, Witzig TE. Inhibition of histone deacetylase overcomes rapamycin-mediated resistance in diffuse large B-cell lymphoma by inhibiting Akt signaling through mTORC2. *Blood.* 2009; 114:2926–35. [PubMed: 19641186]
32. Dibble CC, Asara JM, Manning BD. Characterization of Rictor phosphorylation sites reveals direct regulation of mTOR complex 2 by S6K1. *Mol Cell Biol.* 2009; 29:5657–70. [PubMed: 19720745]
33. Sugiyama T, Kamura T, Kigawa J, Terakawa N, Kikuchi Y, Kita T, et al. Clinical characteristics of clear cell carcinoma of the ovary: a distinct histologic type with poor prognosis and resistance to platinum-based chemotherapy. *Cancer.* 2000; 88:2584–9. [PubMed: 10861437]
34. Behbakht K, Sill MW, Darcy KM, Rubin SC, Mannel RS, Waggoner S, et al. Phase II trial of the mTOR inhibitor, temsirolimus and evaluation of circulating tumor cells and tumor biomarkers in persistent and recurrent epithelial ovarian and primary peritoneal malignancies: a Gynecologic Oncology Group study. *Gynecol Oncol.* 2011; 123:19–26. [PubMed: 21752435]
35. Hietakangas V, Cohen SM. TOR complex 2 is needed for cell cycle progression and anchorage-independent growth of MCF7 and PC3 tumor cells. *BMC Cancer.* 2008; 8:282. [PubMed: 18831768]
36. Bashir T, Cloninger C, Artinian N, Anderson L, Bernath A, Holmes B, et al. Conditional astroglial Rictor overexpression induces malignant glioma in mice. *PLoS One.* 2012; 7:e47741. [PubMed: 23077666]
37. Chresta CM, Davies BR, Hickson I, Harding T, Cosulich S, Critchlow SE, et al. AZD8055 is a potent, selective, and orally bioavailable ATP-competitive mammalian target of rapamycin kinase inhibitor with in vitro and in vivo antitumor activity. *Cancer Res.* 2010; 70:288–98. [PubMed: 20028854]
38. Shi Y, Yan H, Frost P, Gera J, Lichtenstein A. Mammalian target of rapamycin inhibitors activate the AKT kinase in multiple myeloma cells by up-regulating the insulin-like growth factor receptor/

- insulin receptor substrate-1/phosphatidylinositol 3-kinase cascade. *Mol Cancer Ther.* 2005; 4:1533–40. [PubMed: 16227402]
39. Gupta M, Ansell SM, Novak AJ, Kumar S, Kaufmann SH, Witzig TE. Inhibition of histone deacetylase overcomes rapamycin-mediated resistance in diffuse large B-cell lymphoma by inhibiting Akt signaling through mTORC2. *Blood.* 2009; 114:2926–35. [PubMed: 19641186]
  40. Cloughesy TF, Yoshimoto K, Nghiemphu P, Brown K, Dang J, Zhu S, et al. Antitumor activity of rapamycin in a Phase I trial for patients with recurrent PTEN-deficient glioblastoma. *PLoS Med.* 2008; 5:e8. [PubMed: 18215105]

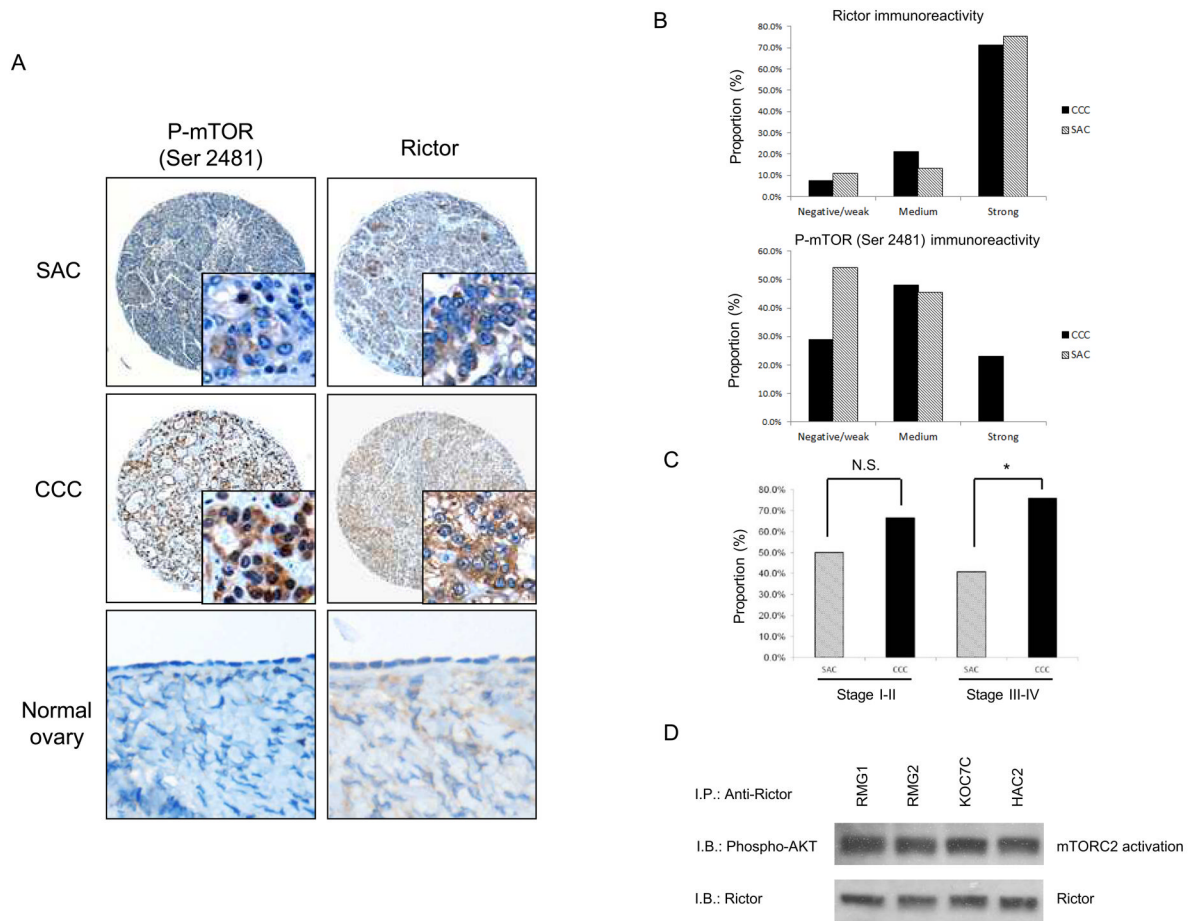


**Figure 1. mTORC2 is frequently expressed and activated in ovarian clear cell carcinomas**  
 Ovarian cancer tissue microarrays and normal ovarian tissues were stained with either anti-Rictor or anti-phospho-mTOR (Ser2481) antibodies. **A**, representative photographs of ovarian tissue microarray cores. Magnifications: x100, and x400 (inset). **B**, histogram indicating immunoreactivity profile. **C**, histogram indicating immunostaining profile by clinical stage. Proportion indicates proportion of medium/strong-staining tumors. \*,  $p < 0.05$ . **D**, mTORC2 activation status in four ovarian CCC cell lines. CCC cells were serum-starved overnight, after which the mTORC2 activity was determined by *in vitro* kinase assay. Briefly, the cell lysates were incubated with anti-Rictor antibody followed by incubation with protein A-agarose. Immunocomplexes were incubated in kinase reaction buffer, and phospho-AKT and Rictor were detected by Western blotting.

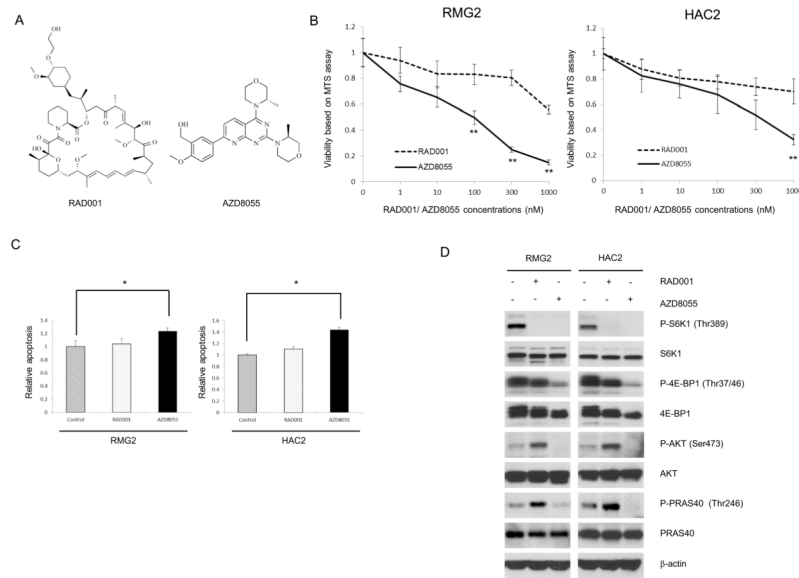


### Figure 2. *In vitro* growth-inhibitory effect of AZD8055 on CCC cell lines

**A**, Chemical structures of RAD001 and AZD8055. **B**, Sensitivity of CCC cells to AZD8055 or RAD001. CCC cells were treated with the indicated concentrations of AZD8055 or RAD001 in the presence of 5% FBS for 72 h. Cell viability was assessed by MTS assay. Points, mean; bars, SD (\*\*, significantly different between RAD001-treated and AZD8055-treated cells at given drug concentration;  $p < 0.01$ ). **C**, AZD8055, but not RAD001, induces apoptosis in ovarian CCC cells. RMG2 and HAC2 cells were treated with 10 nM AZD8055 or 10 nM RAD001 for 24 h in the presence of 5% FBS. The cells were lysed, and DNA fragmentation was examined. Columns, mean; bars, SD. \*,  $P < 0.05$ . **D**, The effect of AZD8055 or RAD001 on the phosphorylation of p70S6K, 4E-BP1, AKT, and PRAS40 *in vitro*. RMG2 and HAC2 cells were treated with 10 nM AZD8055 or 10 nM RAD001 for 6 h in the presence of 5% FBS. Cells were harvested, and equivalent amounts (30  $\mu$ g) of protein were subjected to SDS-PAGE and blotted with various antibodies.

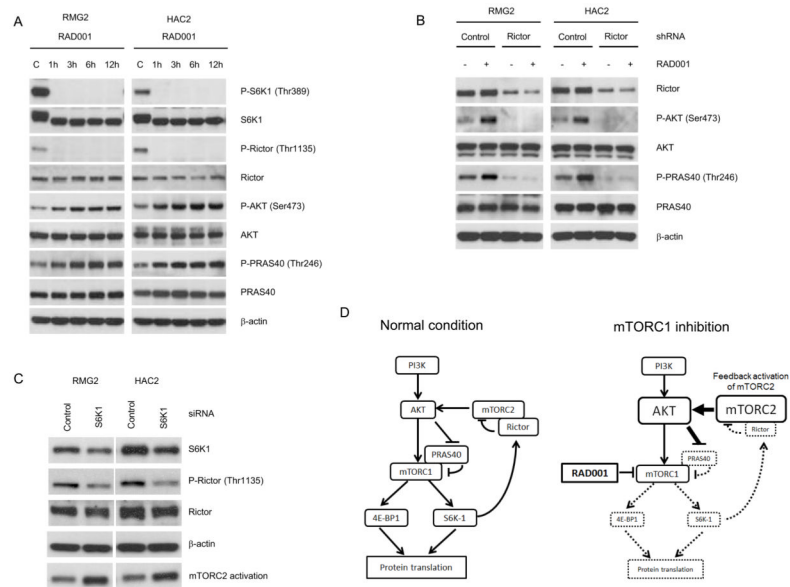


### Figure 3. Inhibition of mTORC1 by RAD001 induces mTORC2-mediated phosphorylation of AKT-PRAS40 signaling in CCC cells

**A**, RAD001 attenuates the phosphorylation of Rictor at Thr1135, which results in increased phosphorylation of AKT and PRAS40 in CCC cells. RMG2 and HAC2 cells were treated with 10 nM AZD8055 or 10 nM RAD001 for the indicated times in the presence of 5% FBS. **B**, Suppression of Rictor by shRNA inhibits RAD001-induced AKT phosphorylation. RMG2 and HAC2 cells plated in 6-well plates were transfected with 20nM control or Rictor shRNA. After 48 h, cells were treated with 10 nM AZD8055 or 10 nM RAD001 for 6 h in the presence of 5% FBS. Cells were harvested, lysed, and equivalent amounts (30  $\mu$ g) of protein were subjected to SDS-PAGE and blotted with various antibodies. **C**, Effect of S6K1 knockdown by siRNA on Rictor phosphorylation and mTORC2 activation. RMG2 and HAC2 cells plated in 6-well plates were transfected with 100 pmol control or S6K1 siRNA. After 48 h, cells were harvested, lysed, and equivalent amounts (30  $\mu$ g) of protein were subjected to SDS-PAGE and blotted with various antibodies. mTORC2 activity was determined by *in vitro* kinase assay as described in “Materials and Methods”. **D**, Model of mTORC1-inhibition mediated feedback activation of AKT. In a normal condition, S6K1 directly phosphorylates Rictor on Thr1135 which negatively regulates the ability of mTORC2 to phosphorylate AKT. mTORC1-inhibition by RAD001 triggers negative feedback mechanisms resulting in mTORC2-mediated phosphorylation of AKT-PRAS40.



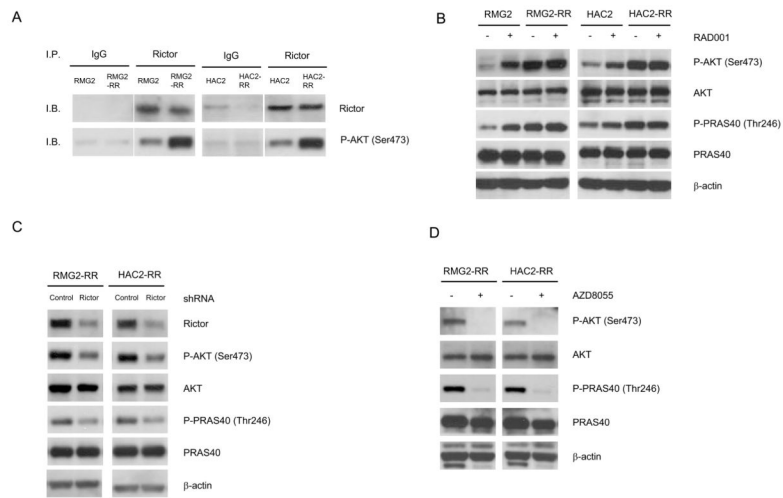


**Figure 4. mTORC2-mediated phosphorylation of AKT-PRAS40 signaling is responsible for resistance to RAD001**

**A**, mTORC2 activation in RAD001-sensitive parental and RAD001-resistant CCC cells. RMG2, HAC2, RMG2-RR, and HAC2-RR cells were serum-starved overnight, after which mTORC2 activation was determined by *in vitro* kinase assay. **B**, Increased phosphorylation of AKT-PRAS40 signaling in RAD001-resistant cells compared to RAD001-sensitive cells. RMG2, HAC2, RMG2-RR, and HAC2-RR cells were serum starved overnight. Cells were harvested, lysed, and then equivalent amounts (30  $\mu$ g) of protein were subjected to SDS-PAGE and blotted with various antibodies. **C**, Suppression of Rictor by shRNA leads to the decreased phosphorylation of AKT and PRAS40 in RAD001-resistant CCC cells. RMG2-RR and HAC2-RR cells plated in 6-well plates were transfected with 20 nM control or Rictor shRNA and evaluated after 48 h. **D**, Treatment with AZD8055 attenuated the phosphorylation of AKT and PRAS40 in RAD001-resistant CCC cells. RMG2-RR and HAC2-RR cells were treated with 10 nM AZD8055 for 6 h. Cells were harvested, lysed, and then equivalent amounts (30  $\mu$ g) of protein were subjected to SDS-PAGE and blotted with various antibodies.

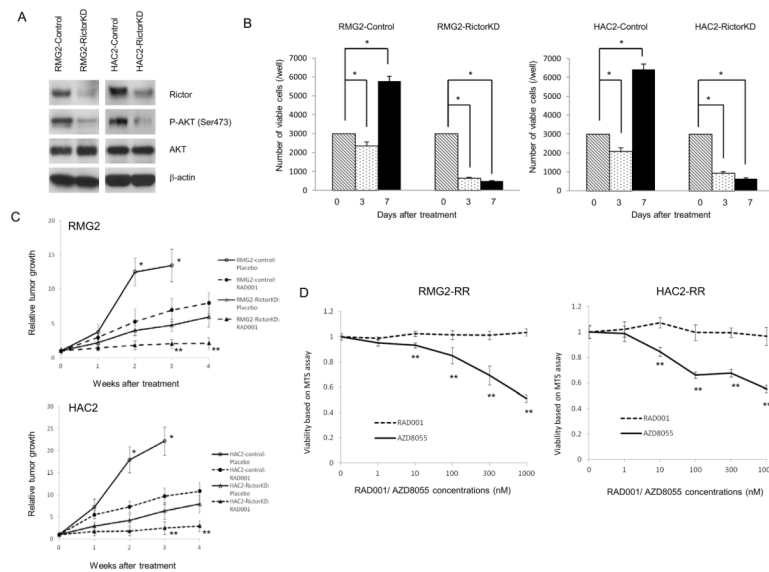


**Figure 5. Inhibition of mTORC2 prevents CCC cells from acquiring resistance to RAD001**  
**A**, Establishment of CCC cell lines stably transfected with control shRNA or Rictor shRNA. Note that knockdown of Rictor results in decreased AKT activity. **B**, Inhibition of mTORC2 activity prevents CCC cells from acquiring resistance to RAD001 *in vitro*. CCC cells stably transfected with control shRNA or Rictor shRNA were seeded into 96-well plates at a density of  $3 \times 10^3$ /well. The cells were then treated with 100 nM RAD001 in the presence of 5% FBS. Cell growth was examined at day 3 and day 7 by cell counting as described in “Materials and Methods,” and the results are shown. Points, mean; bars, SD (\*,  $P < 0.05$ ). **C**, Inhibition of mTORC2-AKT activity during the course of RAD001 treatment prevents CCC cells from acquiring resistance to RAD001 *in vivo*. Athymic nude mice inoculated with CCC cells were administered placebo or 2.5 mg/kg RAD001 every 2 days for 4 weeks. Graphs are depicting weekly tumor volumes ( $\text{mm}^3$ ) for each treatment group. Points, mean; bars, SD (\*, \*\*, significantly different from the RAD001-treated or Rictor shRNA transfected tumors;  $P < 0.05$ ). **D**, Effect of AZD8055 on proliferation of RAD001-resistant CCC cells *in vitro*. RAD001-resistant (RMG2-RR and HAC2-RR) cells were treated with the indicated concentrations of AZD8055 or RAD001 in the presence of 5% FBS for 72 h. Cell viability was assessed by MTS assay. Points, mean; bars, SD (\*\*,  $p < 0.01$ ).

**Table 1**

Correlation between the phospho-mTOR expression and phospho-AKT expression.

	<b>P-AKT medium/strong</b>	<b>P-AKT negative/weak</b>
P-mTOR medium/strong	28	9
P-mTOR negative/weak	5	10